

# Measurements of $R = \frac{L}{T}$ and the Separated Longitudinal and Transverse Structure Functions in the Nucleon Resonance Region

Y. Liang,<sup>1,7</sup> M. E. Christy,<sup>7</sup> A. Ahmidouch,<sup>14</sup> C. S. Amsler,<sup>19</sup> J. Arrington,<sup>2</sup> R. Asaturyan,<sup>23</sup> S. Avery,<sup>7</sup> O. K. Baker,<sup>7,19</sup> D. H. Beck,<sup>8</sup> H. P. Blok,<sup>21</sup> C. W. Bodnar,<sup>8</sup> W. Boeglin,<sup>4,19</sup> P. Bosted,<sup>1,19</sup> M. Bouwhuis,<sup>8</sup> H. Breyer,<sup>9</sup> D. S. Brown,<sup>9</sup> A. Bruehl,<sup>10</sup> R. D. Carlini,<sup>19</sup> J. Cha,<sup>12</sup> N. S. Chant,<sup>9</sup> A. Cochran,<sup>7</sup> L. Cole,<sup>7</sup> S. Danagoulian,<sup>14</sup> D. B. Day,<sup>20</sup> J. D. Dunne,<sup>12</sup> D. Dutta,<sup>10</sup> R. Ent,<sup>19</sup> H. C. Fenker,<sup>19</sup> B. Fox,<sup>3</sup> L. Gan,<sup>7</sup> H. Gao,<sup>10</sup> K. Garrow,<sup>19</sup> D. Gaskell,<sup>2,16</sup> A. Gasparian,<sup>7</sup> D. F. Geesaman,<sup>2</sup> R. Gilman,<sup>18,19</sup> P. L. J. Gueye,<sup>7</sup> M. Harvey,<sup>7</sup> R. J. Holt,<sup>8</sup> X. Jiang,<sup>18</sup> M. Jones,<sup>19</sup> C. E. Kappel,<sup>7,19</sup> E. Kinney,<sup>3</sup> W. Lorenzon,<sup>11</sup> A. Lung,<sup>19</sup> D. J. Mack,<sup>19</sup> P. M. Arkowitz,<sup>4,19</sup> J. W. Martin,<sup>10</sup> K. M. McIlhany,<sup>10</sup> D. McKeen,<sup>13</sup> D. Meekins,<sup>5,19</sup> M. A. Miller,<sup>8</sup> R. G. Miller,<sup>10</sup> J. H. Mitchell,<sup>19</sup> H. Mkrtychyan,<sup>23</sup> B. A. Mueller,<sup>2</sup> A. Nathan,<sup>8</sup> G. Niculescu,<sup>15</sup> I. Niculescu,<sup>6</sup> T. G. O'Neill,<sup>2</sup> V. Papavassiliou,<sup>13,19</sup> S. F. Pate,<sup>13,19</sup> R. B. Piercy,<sup>12</sup> D. Potterveld,<sup>2</sup> R. D. Ransom,<sup>18</sup> J. Reinhold,<sup>4,19</sup> E. Rollinde,<sup>19,22</sup> O. Rondon,<sup>20</sup> P. Roos,<sup>9</sup> A. J. Sarty,<sup>5</sup> R. Sawasta,<sup>14</sup> E. C. Schulte,<sup>8</sup> E. Segbe Ayie,<sup>7</sup> C. Smith,<sup>20</sup> S. Stepanyan,<sup>23</sup> S. Strauch,<sup>18</sup> V. Tadevosyan,<sup>23</sup> L. Tang,<sup>7,19</sup> R. Teulent,<sup>9,19</sup> V. Tavaskis,<sup>7,19</sup> A. Uzzle,<sup>7</sup> W. F. Vulcan,<sup>19</sup> S. A. Woodward,<sup>19</sup> F. Xiong,<sup>10</sup> L. Yuan,<sup>7</sup> M. Zeier,<sup>20</sup> B. Zihlmann,<sup>20</sup> and V. Ziskin<sup>10</sup>.

<sup>1</sup> American University, Washington, D.C. 20016

<sup>2</sup> Argonne National Laboratory, Argonne, Illinois 60439

<sup>3</sup> University of Colorado, Boulder, Colorado 80309

<sup>4</sup> Florida International University, University Park, Florida 33199

<sup>5</sup> Florida State University, Tallahassee, Florida 32306

<sup>6</sup> The George Washington University, Washington, D.C. 20052

<sup>7</sup> Hampton University, Hampton, Virginia 23668

<sup>8</sup> University of Illinois, Champaign-Urbana, Illinois 61801

<sup>9</sup> University of Maryland, College Park, Maryland 20742

<sup>10</sup> Massachusetts Institute of Technology, Cambridge, Massachusetts 02139

<sup>11</sup> University of Michigan, Ann Arbor, Michigan 48109

<sup>12</sup> Mississippi State University, Mississippi State, Mississippi 39762

<sup>13</sup> New Mexico State University, Las Cruces, New Mexico 88003

<sup>14</sup> North Carolina A & T State University, Greensboro, North Carolina 27411

<sup>15</sup> Ohio University, Athens, Ohio 45071

<sup>16</sup> Oregon State University, Corvallis, Oregon 97331

<sup>17</sup> Rensselaer Polytechnic Institute, Troy, NY 12180

<sup>18</sup> Rutgers University, New Brunswick, New Jersey 08855

<sup>19</sup> Thomas Jefferson National Accelerator Facility, Newport News, Virginia 23606

<sup>20</sup> University of Virginia, Charlottesville, Virginia 22901

<sup>21</sup> Vrije Universiteit, 1081 HV Amsterdam, The Netherlands

<sup>22</sup> College of William and Mary, Williamsburg, Virginia 23187

<sup>23</sup> Yerevan Physics Institute, 375036, Yerevan, Armenia

(January 13, 2019)

We report on a detailed study of longitudinal strength in the nucleon resonance region, presenting new results from inclusive electron-proton cross sections measured at Jefferson Lab Hall C in the four-momentum transfer range  $0.2 < Q^2 < 5.5 \text{ GeV}^2$ . The data have been used to accurately perform over 170 Rosenbluth-type longitudinal / transverse separations. The precision  $R = \frac{L}{T}$  data are presented here, along with the first separate values of the inelastic structure functions  $F_1$  and  $F_L$  in this regime. The resonance longitudinal component is found to be significant. With the new data, quark-hadron duality is observed above  $Q^2 = 1 \text{ GeV}^2$  in the separated structure functions independently.

The description of hadrons and their excitations in

terms of elementary quark and gluon constituents is one of the fundamental challenges in physics today. Considerable information on nucleon structure has been extracted over the past few decades from separations of inclusive lepton-nucleon cross sections into longitudinal and transverse structure functions. The original experimental observation [1] of the smallness of the ratio  $R = \frac{L}{T}$ , the ratio of the contributions to the measured cross section from longitudinally and transversely polarized virtual-photon scattering, respectively, as measured in deep inelastic scattering (DIS) provided the first evidence of the fundamental spin-1/2 nature of the partons. Since that time, separated structure functions have been measured in DIS over a wide range of four-momentum transfer,  $Q^2$ , and Bjorken scaling variable  $x = Q^2/2M$ , where  $= E - E^0$  is the electron energy transfer, and  $M$  is the

proton mass.

The quantity  $R$  is expressed in terms of the fundamental nucleon structure functions  $F_1$  (purely transverse),  $F_L$  (purely longitudinal), and  $F_2$  (combined longitudinal and transverse) as follows:

$$R = \frac{F_L}{T} = \frac{F_L}{2xF_1} = \frac{F_2}{2xF_1} = 1 + \frac{4M^2x^2}{Q^2} \quad 1: \quad (1)$$

Precision measurements of  $R$  are necessary for several fundamental measurements. Extractions of the structure function  $F_2$ , or of the purely longitudinal or transverse structure functions,  $F_L$  and  $F_1$ , from cross section measurements depend on assumptions for  $R$ . The uncertainties introduced by this assumption are highly dependent, where  $\epsilon$  is the relative longitudinal polarization of the virtual photon in the electron-nucleon scattering process. Uncertainties in the separation of unpolarized structure functions also have a direct impact on the extraction of the spin structure functions from spin-asymmetry measurements in electron scattering.

Very few measurements of  $R$  have been made in the nucleon resonance region. Here, the quantity and precision of the existing data (prior to this work) was such that it was impossible to study either the mass-squared ( $W^2$ ) or  $Q^2$  dependences of the separated longitudinal and transverse resonant structure. In a resonance excitation probed at moderate momentum transfer, large values of  $R$  and, correspondingly,  $F_L$ , are possible, due to gluon exchanges between the quarks. These effects, as well as the longitudinal character of individual resonances, are accessible via precision measurements of  $R$ .

In perturbative Quantum Chromodynamics (pQCD),  $F_L \propto \epsilon$ , and thus  $R$  is expected to decrease logarithmically with increasing  $Q^2$  [24]. At low  $Q^2$ ,  $Q^2$ -type dynamical higher twist power corrections, interactions in which the struck quark exchanges a gluon with one of the spectator quarks in the scattering process, are expected to be a significant contribution to  $R$ . Additionally, kinematic higher twist effects originating from the binding of the quarks in the nucleon (target mass effects), are expected to be large. It has been previously reported [6] that  $R$  measured at intermediate  $Q^2$  in the DIS regime [1,5,7] is higher than next-to-leading-order pQCD predictions, even with the inclusion of target mass corrections. This enhanced strength in  $R$  relative to pQCD was argued to be an observation of non-perturbative higher twist effects [6,7].

In contrast, recent quantitative studies [8] of quark-hadron duality in the structure function  $F_2$  suggest that, even in the resonance region, non-perturbative dynamical higher twist effects tend to be small for  $Q^2$  as low as  $1 \text{ GeV}^2$  when the structure function is averaged over any of the prominent resonance regions. That is, even though the function exhibits resonance (hadronic) structure, it tends to average to a global scaling curve consis-

tent with expectations from DIS data and perturbative QCD (hence the term quark-hadron duality).

The results presented here represent the first detailed study of longitudinal strength in the full nucleon resonance region, to investigate nucleon resonance structure, nucleon structure function behavior, and quark-hadron duality.

The experiment (E 94-110) ran in the summer of 1999 in Hall C at Jefferson Lab. An electron beam with a near constant current of  $60 \text{ A}$  was provided by the CEBAF accelerator with seven different energies ranging from  $1.2 \text{ GeV}$  to  $5.5 \text{ GeV}$ . Incident electrons were scattered from a 4-cm-long liquid hydrogen target and detected in the High Momentum Spectrometer (HMS), over a scattered electron angle,  $\theta$ , range  $12.9^\circ < \theta < 79.9^\circ$ . To account for backgrounds from  $\pi^0$  production and its subsequent decay into two photons and then electron-positron pairs, positrons were measured in the Short Orbit Spectrometer (SOS) and also intermittently in the HMS. Other backgrounds included electron scattering from the aluminum walls of the cryogenic target cell, as well as electroproduced negatively charged pions. Events from the former were subtracted by performing substitute empty target runs, while events from the latter were identified and removed by use of both a gas Cherenkov counter and an electromagnetic calorimeter. For more details regarding the analysis and the standard Hall C apparatus employed in this experiment, see Ref. [9]. Additional discussion may also be found in Reference [10], a recent analysis of elastic scattering data from this experiment.

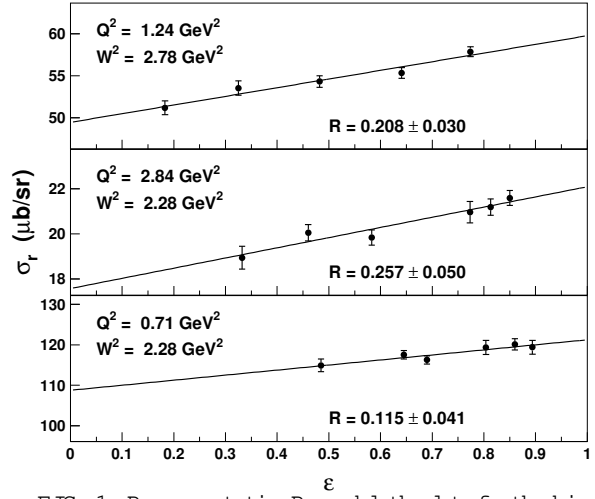


FIG. 1. Representative Rosenbluth plots for the kinematics indicated, as described in the text.

The inclusive double differential cross section for each energy and angle bin within the spectrometer acceptance was determined from

$$\frac{d}{dE^0} = \frac{Y_{\text{corr}}}{L} \frac{1}{E^0}; \quad (2)$$

where  $(E^0)$  is the bin width in solid angle (scat-

tered energy),  $L$  is the total integrated luminosity, and  $Y_{\text{corr}}$  is the measured electron yield after correcting for detector inefficiencies, background events, and radiative corrections. The latter include the bremsstrahlung, vertex corrections, and loop diagrams standard to electron scattering experiments. No corrections were made for higher order radiative processes involving two photon exchange, since there exists no reliable inelastic calculation for such effects. However, the large kinematic coverage in  $W^2$ , and  $Q^2$  of this experiment demonstrated minimal (less than 2% [11]) non-linear dependence of the reduced cross section.

The width of the energy bins was varied with the kinematics such that the corresponding bin width in  $W^2$  was held constant at  $0.05 \text{ GeV}^2$ , where  $W^2 = M^2 + 2M$ .  $Q^2$  is the reconstructed mass-squared of the recoiling hadronic system. For each energy bin, a weighted average cross section over within the spectrometer acceptance was obtained after using a model to correct for the angular variation of the cross section from the central angle value. In order to minimize dependence on the model used to compute both this and the radiative correction, the following iterative procedure was employed: a model was used to compute the corrections; the data thus obtained were fit to obtain a new model; and this resultant new model was then employed to recompute the original corrections. These steps were repeated until the fitting yielded no further changes. It was also verified that the final cross sections were independent of the starting model within 0.6%. A positive byproduct of this approach is the availability of a new resonance region which describes the data here presented [12].

Typical cross section statistical uncertainties per energy bin were less than 1% with systematic errors, uncorrelated in  $Q^2$ , of 1.6%. The total systematic scale uncertainty in the cross section measurements was 1.9%. The full cross section sample consisted of 32 scans across the mass-squared range  $M^2 < W^2 < 4 \text{ GeV}^2$ . Measurements at over 1,000 distinct  $W^2, Q^2$  and points were obtained, allowing for longitudinal / transverse separations to be performed at over 170 fixed  $W^2, Q^2$  values.

The extractions of purely longitudinal and transverse cross sections and structure functions were accomplished via the Rosenbluth technique [13], where measurements are made over a range in  $x$ ,  $Q^2$ , and the reduced cross section,  $r = d = T + L = T(1 + "R")$  is fit linearly with  $x$ . Here,  $T$  is the transverse virtual photon flux in the electron-nucleon scattering process. Both  $r$  and  $L$  were calculated from measured kinematic variables. The intercept of such a fit gives the transverse cross section  $T$  (and therefore the structure function  $F_1(x; Q^2)$ ), while the slope gives the longitudinal cross section  $L$ , from which can be extracted the structure functions  $R(x; Q^2)$  and  $F_L(x; Q^2)$ . Because  $R$  is determined by the slope of the  $r$ , relative to  $T$ , the uncertainty in the extracted value of  $R$  (and likewise,  $F_L$ ) is

dominated by the uncorrelated uncertainties in the cross sections versus  $x$ . Prior to a separation being performed, data covering a  $Q^2$  range of  $0.5 \text{ GeV}^2$  and  $W^2$  range of  $0.05 \text{ GeV}^2$  for  $W^2 < 3.0 \text{ GeV}^2$  and  $0.10 \text{ GeV}^2$  for  $W^2 > 3.0 \text{ GeV}^2$  were brought to a central value using a fit. Multiple fits were utilized to assess the uncertainty in this step, which was typically less than 3%. Separations were not performed if this kinematic correction was larger than 60%. Typical example Rosenbluth plots are shown in Fig. 1.

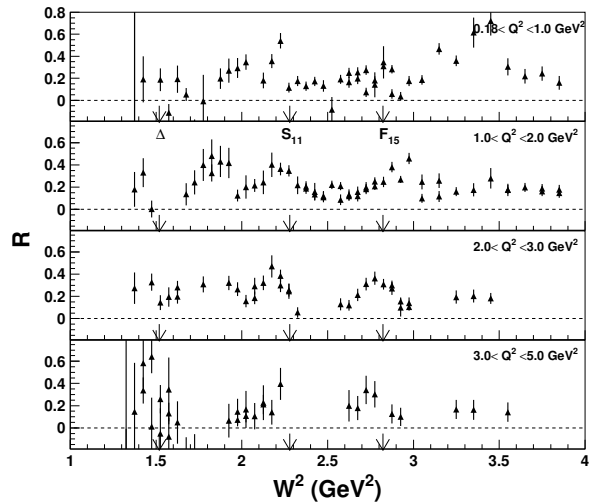


FIG. 2. Measurements of  $R = L/T$ , as a function of  $W^2$ , for the  $Q^2$  ranges indicated. The error bars shown represent both the statistical and uncorrelated systematic uncertainties, however the former are negligible in comparison to the latter.

Values obtained for  $R$  are plotted versus  $W^2$  in Fig. 2 for the  $Q^2$  ranges indicated. Because the data were obtained at fixed spectrometer angles and electron beam energies, while varying the central spectrometer momenta, each missing mass spectrum covered a range in  $Q^2$ . It is clear from the mass enhancements in the data that  $R$  exhibits resonant structure, and that this variation with  $W^2$  can be quite large. This is the first observation of such structure, contradicting the typical assumption in inclusive analyses that the resonance contribution to  $R$  is small or negligible [14,15] in the excitation of resonances.

The almost twenty well-established nucleon resonances with masses below 2 GeV give rise to only three distinct enhancements in the unseparated inclusive electron scattering cross section and, of the three, only the first (the lowest mass  $P_{33}(1232)$ ,  $\Delta$ ) state is not a superposition of overlapping resonant states. The second enhancement region is often referred to as the  $S_{11}$ , as the unseparated cross section here is dominated above  $Q^2 = 1 \text{ GeV}^2$  by the ground state  $S_{11}(1535)$  resonance, even though there are overlapping candidate states. In  $R$ , however, the situation appears to be different. There is a prominent peak at  $W^2 = 2.2 \text{ GeV}^2$ , somewhat below the  $S_{11}$  dominated mass region.

While the resonance region exhibits smaller and rather constant values,  $R$  is nonetheless not negligible here, nor does it appear to diminish over the  $Q^2$  range of this experiment. Yet, the spin- $\frac{1}{2}$  required for this positive parity isospin  $I = \frac{3}{2}$  excitation suggests that it will be purely transverse. Recent measurements from Hall B at JLab [16] indicate only a small longitudinal resonant component. Therefore, it is probable that the  $R$  here observed indicates a substantial background contribution in this regime.

The data also exhibit resonance behavior in the longitudinal and transverse structure functions separately, as shown in Fig. 3. This does not necessarily follow from the resonance behavior of the ratio  $R = F_L/F_T$  shown above, which could be caused by a cross section that is resonant in only the transverse channel. Moreover, not only do the data demonstrate significant longitudinal resonance structure, but the  $W$ -dependence of  $F_L$  is larger than that of  $2xF_1$  above  $Q^2 = 1 \text{ GeV}^2$ .

The peak observed in  $R$  at  $W^2 = 2.2 \text{ GeV}^2$  in Fig. 2 below the  $S_{11}$  is particularly notable in the  $F_L$  longitudinal channel. This mass is close to that of the elusive Roper resonance,  $P_{11}(1440)$ , the electroproduction of which is a topic of much interest [17{21].

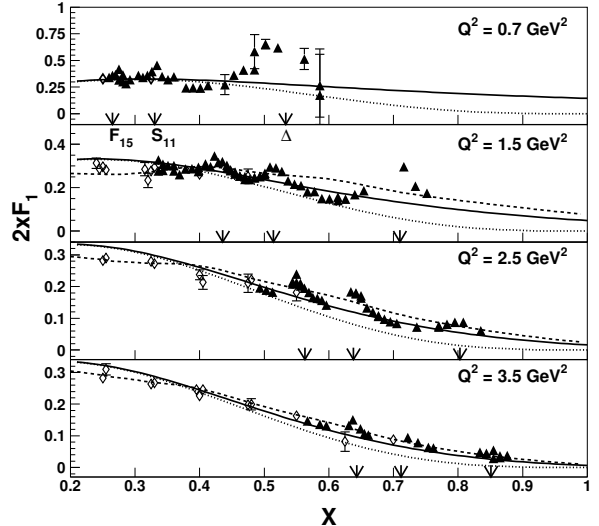
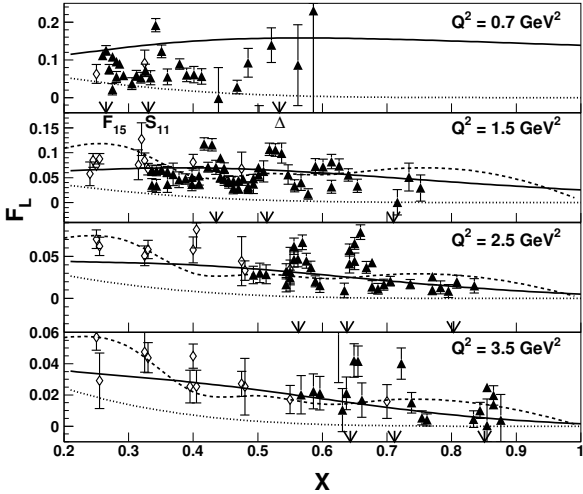


FIG. 3. The longitudinal nucleon structure function  $F_L$  (top), and transverse nucleon structure function  $2xF_1$  (bottom), measured in the resonance region (triangles) as a function of  $x$ , compared with existing DIS measurements from SLAC (diamonds). The curves are from A lekhin (dashed), and M RST with (solid) and without (dotted) target mass effects included, as described in the text. The prominent resonance mass regions are indicated by arrows. The error bars shown represent both the statistical and systematic uncertainties, with the latter being dominant.

A precise extraction of information on individual resonances, such as transition form factors, from this inclusive data must involve a detailed fitting study. At lower values of  $Q^2 < 1 \text{ GeV}^2$ , unitary isobar fits like MAID [22] give quite definite and accurate predictions based on single pion, two pion, eta, and kaon decay channels for resonances below  $W^2 < 4 \text{ GeV}^2$ . At the higher  $Q^2$  values of the data presented here, however, multipion effects, tails of higher mass resonances, and non-resonant components are very significant and therefore such fits tend to undercut the data by factors of two or more [23].

Also presented with the resonance region data in Fig. 3 are the predominantly DIS ( $W^2 > 4 \text{ GeV}^2$ ) data from Rosenbluth separations performed at SLAC [7,6]. Where overlapping, the two data sets are in agreement, providing additional confidence in the achievement of the demanding precision required for these experiments. In all cases, there is a smooth transition between the resonance and DIS data in both  $x$  and  $Q^2$ .

The curves shown are next-to-next-to leading order, from A lekhin [24], including target mass effects according to [26], and from a recent M RST analysis [25] both with and without target mass effects according to [27]. Both of these are parton distribution function based parameterizations of deep inelastic data. However, M RST includes data from other sources as well. A lekhin's calculations are valid only down to  $Q^2 = 1 \text{ GeV}^2$ .

It is clear that some prescription for target mass effects is required to describe the data. However, for  $Q^2 > 1$

$\text{GeV}^2$ , no additional non-perturbative description seems necessary to describe the average behavior of the resonance region. The resonances oscillate around the scaling curves. Furthermore, this is true for a range of different  $Q^2$  values, indicating that the scaling curve describes as well the average  $Q^2$  dependence of the resonance regime. This is consistent with quark-hadron duality, and may be counted as the first observation of duality in the separated transverse and longitudinal structure functions.

In summary, we have reported results from a first detailed study of longitudinal strength in the nucleon resonance region. Contrary to most transition form factor assumptions, the resonant longitudinal component is found to be substantial. Furthermore, the  $W^2$ -dependence of the longitudinal structure function is more pronounced than the transverse. Significant strength is observed between the  $S_{11}$  and  $P_{33}$  resonance mass regions in the longitudinal channel. Separated measurements of the inelastic structure functions  $F_1$  and  $F_L$  are presented, allowing for a first observation of quark-hadron duality in these distinct functions independently.

This work was supported in part by research grants 0099540 and 9633750 from the National Science Foundation. We thank the Jefferson Lab Hall C scientific and engineering staff for their outstanding support. The Southeastern Universities Research Association operates the Thomas Jefferson National Accelerator Facility under the U.S. Department of Energy contract DEAC05-84ER40150.

- [18] Z. p. Li, V. Burkert and Z. j. Li, *Phys. Rev. D* **46**, 70 (1992)
- [19] S. R. Beane and U. van Kolck, *nucl-th/0212039*
- [20] R. D. M. atheus, F. S. Navarra, M. Nielsen, R. Rodrigues da Silva and S. H. Lee, *Phys. Lett. B* **578**, 323 (2004)
- [21] R. L. Jaffe and F. W. Ilczek, *Phys. Rev. Lett.* **91**, 232003 (2003)
- [22] W. T. Chiang, S. N. Yang, L. Tiator and D. D. Redsel, *Nucl. Phys. A* **700**, 429 (2002); G. Knochlein, D. D. Redsel and L. Tiator, *Z. Phys. A* **352**, 327 (1995)
- [23] M. E. Christy, Prepared for N STAR 2002 Workshop on the Physics of Excited Nucleons, Pittsburgh, Pennsylvania, 9-12 Oct 2002
- [24] S. A. Lezhin, *Phys. Rev. D* **68**, 014002 (2003)
- [25] A. D. Martin, R. G. Roberts, W. J. Stirling, and R. S. Thorne, *Eur. Phys. J. C* **18**, 117 (2000)
- [26] H. Georgi and H. D. Politzer, *Phys. Rev. Lett.* **36** (1976) 1281; *Erratum* **37** (1976) 68; *Phys. Rev. D* **14**, 1829 (1976)
- [27] R. Barbieri, J. R. Ellis, M. K. Gaillard and G. G. Ross, *Nucl. Phys. B* **117**, 50 (1976)

---

- [1] A. Bodek et al., *Phys. Rev. D* **20**, 1471 (1979)
- [2] G. A. Litarelli and G. M. Martinelli, *Phys. Lett. B* **76B**, 89 (1978)
- [3] R. K. Ellis et al., *Nucl. Phys. B* **207**, 1 (1982)
- [4] R. K. Ellis et al., *Nucl. Phys. B* **212**, 29 (1982)
- [5] L. W. W. Hiltow et al., *Phys. Lett. B* **250** (1990) 193.
- [6] L. H. Tao et al., *Z. Phys. C* **70**, 387 (1996)
- [7] S. Dasu et al., *Phys. Rev. D* **49**, 5641 (1994)
- [8] I. Niculescu et al., *Phys. Rev. Lett.* **85**, 1186 (2000); I. Niculescu et al., *Phys. Rev. Lett.* **85**, 1182 (2000)
- [9] Y. Liang, PhD Thesis, The American University (2003), unpublished
- [10] M. E. Christy et al. [94110 Collaboration], *Phys. Rev. C* **70**, 015206 (2004)
- [11] V. Tavaskis, et al., publication in preparation
- [12] The data and fits are available at [halloweb.jlab.org/resdata](http://halloweb.jlab.org/resdata).
- [13] M. N. Rosenbluth, *Phys. Rev.* **79**, 615 (1956)
- [14] P. Stoler, *Phys. Rept.* **226**, 103 (1993)
- [15] L. M. Stuart et al., *Phys. Rev. D* **58**, 032003 (1998)
- [16] K. Joo et al. [CLAS Collaboration], *arXiv:nucl-ex/0407013* (2004)
- [17] L. Alvarez-Ruso, M. B. Barbaro, T. W. Donnelly and A. Molinari, *Nucl. Phys. A* **724**, 157 (2003)